Bioorganic & Medicinal Chemistry Letters 19 (2009) 1148–1151

Contents lists available at ScienceDirect

Bioorganic & Medicinal Chemistry Letters

journal homepage: www.elsevier.com/locate/bmcl

Synthesis, biological activity and tubulin binding poses of 1-deoxy-9-(*R*)-dihydrotaxane analogs

Tian-Hai Yuan [a], Yi Jiang [b], Xiao-Hong Wang [a], Dian-Long Wang [a], Abhijit Bannerjee [c], Susan Bane [c], James P. Snyder [b], Hai-Xia Lin [a,*]

[a] *Department of Chemistry, Shanghai University, Shanghai 200444, China*
[b] *Department of Chemistry, Emory University, Atlanta, GA 30322, USA*
[c] *Department of Chemistry, Binghamton University, State University of New York, Binghamton, NY 13902, USA*

ARTICLE INFO

Article history:
Received 4 July 2008
Revised 19 December 2008
Accepted 23 December 2008
Available online 27 December 2008

Keywords:
Paclitaxel
1-Deoxybaccatin VI
Conformation
1-Deoxy-9α-dihydrotaxane analog

ABSTRACT

1-Deoxy-9α-dihydrotaxane analogs **9** and **10** were semi-synthesized from 1-deoxybaccatin VI, isolated from *Taxus mairei*, and tested for cytotoxic activity. Taxane **9** is 10-fold less cytotoxic than paclitaxel, while **10** is equally active. In the tubulin polymerization assay (ED_{50} values), **10** is 4-fold less effective than paclitaxel, but 3-fold superior to **9**. These observations can be explained by analysis of the corresponding taxane/β-tubulin complexes.

In spite of the clinical application of paclitaxel 1 and docetaxel 2 as anticancer agents,[1,2] taxoids remain a subject of research for the design of novel anticancer drugs and a more complete knowledge of their interaction with microtubules. Recently, one aspect of taxane study has focused on the treatment of multidrug-resistance (MDR) in cancer cells, largely a manifestation of the overexpression of P-glycoprotein (P-gp).[3] It has been proposed that the ability of C-10 taxane analogs to overcome MDR in vitro is the result of reduced binding affinity for P-glycoprotein.[4] Structure–activity relationship (SAR) studies performed by a number of different groups have demonstrated that the C7–C10 region is quite tolerant to modifications, probably due to the fact that these centers do not interact directly with tublin.[5] Of particular significance, the cytotoxicities of 7-dexoy-9α-dihydro-9,10-isopropylidenedocetaxel 3 and 9β-dihydro-9,10-acetal taxoid 4 were reported to be similar to[6] and more potent[7] than docetaxel, respectively. These reports demonstrate clearly that acetal groups installed at the C-9, C-10 positions of the taxane skeleton promote effective bioactivity.

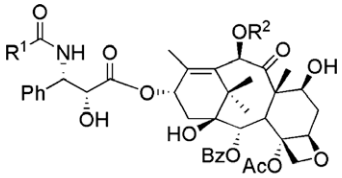

paclitaxel (**1**: R^1 = Ph, R^2 = Ac)
docetaxel (**2**: R^1 = *t*-BuO, R^2 = H)

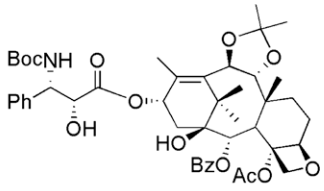

3

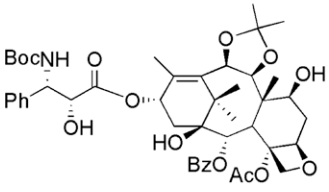

4

1-Deoxybaccatin VI **5** that possesses the typical tetracyclic taxoid core while lacking the C-1 hydroxy group is readily available from

* Corresponding author. Tel.: +86 21 66134854; fax: +86 21 66132797.
E-mail address: haixialin@staff.shu.edu.cn (H.-X. Lin).

0960-894X/$ - see front matter © 2008 Elsevier Ltd. All rights reserved.
doi:10.1016/j.bmcl.2008.12.091

T. mairei.[8] Deoxygenation of the hydroxy group for baccatin III or paclitaxel had been reported to be a difficult procedure.[9] Thus, the development of a method using 1-deoxybaccatin VI as the starting point for preparation of new active taxoids will be of value. Moreover, SAR studies have revealed that the C-1 hydroxy group is not necessary for the activity of paclitaxel.[10] Herein, we report the synthesis and antitumor activities of 1-dexoy-9α-dihydrotaxane analogs. Importantly, we also explore the correlation between the single-crystal X-ray structure of **9** and its binding affinity to microtubules.

As depicted in Scheme 1, the natural taxoid **5** was transformed to **6** upon treatment with hydrazine hydrate in ethanol.[11] The 9,10-dihydroxy moiety of the latter compound was selectively protected with 2,2-dimethoxypropane catalyzed by montmorillonite K10 to give **7** in 97% yield.[11] The next step in the synthesis was introduction of a phenylisoserine side chain selectively at C-13. Treatment of **7** with (4*S*,5*R*)-2,4-diphenyloxazoline-5-carboxylic acid **11** in the presence of DCC-DMAP afforded a good yield of the desired coupling product **8**.[11] The result revealed the reactivity difference between the 7-hydroxyl and 13-hydroxyl groups, contrary to the reaction of 9β-dihydrobaccatin-9,10-acetals with β-lactams in the presence of NaHMDS.[7] Hydrolysis of the cyclic ester **8** with 0.04 N HCl yielded *N*-benzoylphenylisoserinate **9**[11] in good yield. Although 9β-dihydro-3′-furyldocetaxel was not obtained from 9β-dihydro-9,10-isopropylidene-3′-furyldocetaxel by acidic deprotection of the acetal group,[7] we synthesized **10**[11] from **9** by deprotection of the acetonide under acidic conditions using somewhat different from those reported in the literature. Analogs **9** and **10** along with paclitaxel were subsequently evaluated in cytotoxicity assays employing the A 2780 (ovarian carcinoma) and A 549 (human lung carcinoma) cell lines. As reported in Table 1, analog

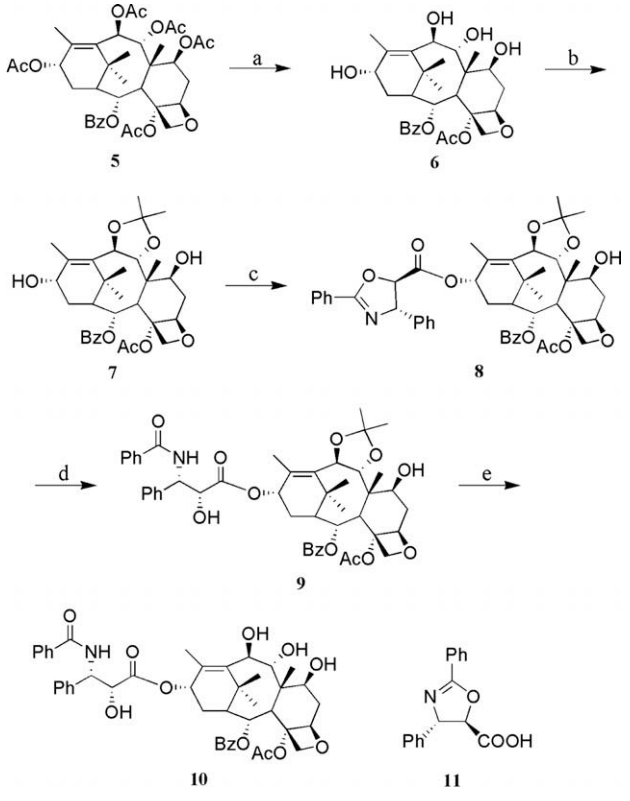

Scheme 1. Reagents and conditions: (a) $NH_2NH_2{\cdot}H_2O$, EtOH, rt, 87%; (b) 2,2-dimethoxypropane, montmorillonite K10, CH_2Cl_2, rt, 97%; (c) **11**, DCC/DMAP, toluene, 83%; (d) 0.04 N HCl, CH_3OH/H_2O, 60–70 °C 67%; (e) 0.04 N HCl, CH_3OH/H_2O, 80–90 °C 95%.

Table 1
Cytotoxicities and tubulin polymerization IC_{50} values for paclitaxel and analogs **9** and **10**

Compound	Cytotoxic activity IC_{50}[a] (ng/mL)		Tubulin polymerization ED_{50}[b] (μM)
	A 2780	A 549	
Paclitaxel	0.13	0.29	0.52 ± 0.02
9	1.54	2.87	5.2 ± 0.4
10	0.11	0.18	1.9 ± 0.3

[a] IC_{50} is described as the concentration of agent required to inhibit cell proliferation to 50% versus untreated cells (incubated at 37 °C for 72 h) determined by the MTT colorimetric microtiter assay.
[b] GTP-tubulin concentration, 10 μM.

10 shows activity comparable to that of paclitaxel, while analog **9** possesses a 10-fold reduced cytotoxicity contrary to what has been previously reported for 7-dexoy-9α-dihydro-9,10-isopropylidene-docetaxel (**3**) and 9β-dihydro-9,10-acetal (**4**) taxoids.[6,7] Consistent with the cytotoxicity data, **10** is 3-fold more potent than **9** in the tubulin polymerization assay, although it is 4-fold less potent than paclitaxel.

Structure–activity studies have shown that minor structural modifications of paclitaxel can lead to significant differences in binding affinity to microtubules. In order to explain the diminished activity of **9**, we have compared its conformational features in the solid state and at the tubulin binding site, the latter a result of computational docking. In the crystal, **9** exists as a 1:1 complex with methanol, the solvent from which the crystal was grown. In the solid state, **9** adopts a conformation (Fig. 1) resulting from intramolecular (1′C=O···H–O2′, O7···H–O6) and intermolecular (O4···H–O6, O2···H–N1, O5′···H–OCH_3) hydrogen bonds along with other weak hydrogen bonds and normal van der Waals interactions. Consequently, the C-3′ phenyl ring is projected away from the taxane core, while the C-3′ benzamide moiety is directed toward the C-2 benzoate group. This orientation is reminiscent of the nonpolar conformer found in the crystal structure of docetaxel[12] and the T-Taxol conformer of β-tubulin-bound paclitaxel.[13] For a more detailed comparison of the C-13 side chain conformations, Table 2 lists selected torsion angles for **9**, docetaxel, paclitaxel

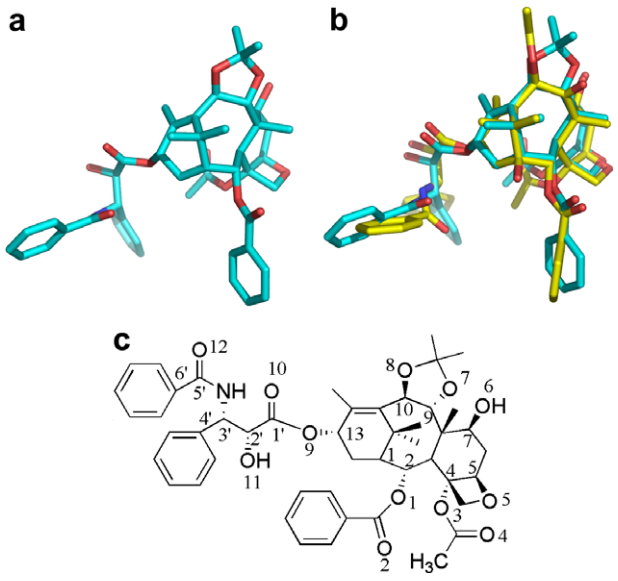

Figure 1. (a) X-ray structure of **9**. One methanol molecule in the unit cell is omitted for the sake of clarity. (b) Superposition of the crystal structure of **9** (cyan) and T-Taxol (yellow). (c) Labeling scheme of selected atoms of **9**.

Table 2
Selected torsion angles (°) for C-13 side chains of **9**, docetaxel, conformer A and B of paclitaxel, and T-Taxol

Torsion angle	**9**	Docetaxel	Paclitaxel A[14]	Paclitaxel B[14]	T-Taxol
C13–O9–C1′–O10	5.0	−6.6	2	4	0.6
C13–O9–C1′–C2′	−177.4	168.0	180	−177	−178.7
O9–C1′–C2′–C3′	68.0	60.2	159	103	55.7
O10–C1′-C2′–O11	8.1	−2.2	93	41	−1.2
C1′–C2′–C3′–N	74.0	56.4	176	179	52.4
O11–C2′–C3′–C4′	78.7	59.5	180	−175	58.5
O11–C2′–C3′–N	−47.6	−64.6	60	61	−67.0
C5′–N–C3′–C2′	−88.9	−141.4	−118	−155	−153.4
C5′–N–C3′–C4′	142.5	97.4	120	83	82.8
C3′–N–C5′–O12	−4.7	12.8	1	−1	−1.0

and T-Taxol. As suggested by the torsion angles, the variations in torsion angles around the C1′–C2′ and C2′–C3′ bonds seem to dominate changes in the orientation of the side chain relative to the core. Comparison of the torsion angles shows that **9** adopts a significantly different conformation of the C-13 side chain relative to the solid state conformers of paclitaxel (PTX), but quite similar to that of docetaxel (DTX) and T-Taxol. The conformation of the C-13 side chain is also characterized by the value of the torsion angle H2′–C2′–C3′–H3′. In the H-atom enhanced crystal structure of **9**, this angle is 77.1°, slightly larger than the 55.4° and 57.3° values in the latter two molecules, respectively. Another significant indicator concerns the distances between the centroids of the C-2 benzoyl phenyl ring and the C-3′ phenyl and benzamido phenyl rings. As revealed by Table 3, these distances for **9** resemble more those of DTX and T-Taxol rather than those found in the solid state for the conformers of PTX. To make a fuller comparison, Figure 1b also depicts superposition of the crystal conformers of **9** and T-Taxol when the baccatin cores are matched. In accordance with the similarity of the ring-to-ring distances, the placements of the C-13 side chains of the two molecules are closely overlapped. Among other things, the comparison suggests that **9** and PTX might be expected to exhibit similar bio-actions. The deviations as represented by Table 1 are discussed below.

In an attempt to examine the possible conformational role of the acetonide functionality in **9** versus its absence in **10**, the structural features of **6** and **7** been also been investigated using single-crystal X-ray diffraction methods.[15] The taxane ring conformation of **7** is nearly identical to that of **6**. Comparison of various torsion angles (C5–C6–C7–C8, C6–C7–C8–C9, C8–C9–C10–C11, C9–C10–C11–C15, C11–C12–C13–C14, C15–C1–C14–C13) show them to differ by no more than 8°. Similarly, the distance between C-5 and C-13 is virtually the same in the two structures (**7**, 5.7; **6**, 5.6 Å). Accordingly, it appears that the acetonide group in **7** does not impart any significant alteration to the baccatin core relative to **6**.

In the context of protein enclosure, we have optimized the geometries of **9** and **10** (MMFF/GBSA/H_2O)[16] and flexibly docked the corresponding conformers with the closest likeness to T-Taxol into the β-tubulin pocket of an M-loop modified protein model 1JFF[17] with the Glide docking program (Fig. 2).[18]

Table 3
The distances between the centroids of the C-2 benzoyl phenyl ring and the C-3′ phenyl and benzamide phenyl rings (Å) for **9**, docetaxel, and paclitaxel X-ray structures and T-Taxol

Distances[a]	**9**	Docetaxel	Paclitaxel		T-Taxol
			A	B	
d_1	7.1	10.7	8.9	5.7	9.4
d_2	10.5	7.2	13.0	11.6	10.0

[a] d_1: the distances between the centroids of the C-2 benzoyl phenyl ring and the C-3′ phenyl ring; d_2: the distances between the centroids of the C-2 benzoyl phenyl ring and the benzamido phenyl ring or *t*-butyl group.

A striking difference between the structures of T-Taxol and **9** in the taxane binding pocket is that the baccatin core of the latter shifts away from the M-loop relative to T-Taxol during the modeling exercise. It appears that one of the 9,10-acetonide methyl groups engages in a steric clash with Arg284 that leads to ligand translation within the binding pocket. One consequence is that the oxetane ring in **9** is separated from Thr276 resulting in loss of hydrogen bonding between the oxygen atom of the oxetane ring and HN-Thr276, while simultaneously causing the compound to sit a bit higher in the binding pocket (Fig. 2). By contrast, the baccatin core of **10** matches that of T-Taxol and retains the H-bond to Thr276. As a result, the docking poses are qualitatively consistent with the results of both cytotoxicity and tubulin polymerization assays as reported in Table 1.

In summary, we have synthesized 1-deoxy-9α-dihydro taxane analogs from 1-deoxybaccatin VI and found that analog **9** based on the 9,10-acetonide taxane skeleton exhibits a 10-fold drop in cytotoxicity in two cell-based assays relative to paclitaxel. On the other hand, the 9,10-diol **10** exhibits activity equal to paclitaxel in the same assays. Tubulin polymerization activities of the two analogs are qualitatively consistent with the observed cytotoxicities. To understand these activity profiles, we solved the crystal structure of **9** and show that it adopts a conformation very close that of T-Taxol, the β-tubulin-bound form of paclitaxel. However, the acetonide appears to cause an unfavorable relocation of **9** in the tubulin binding cleft, disfavoring the compound's binding affinity relative to **10**. The T-Taxol conformation has proven to be

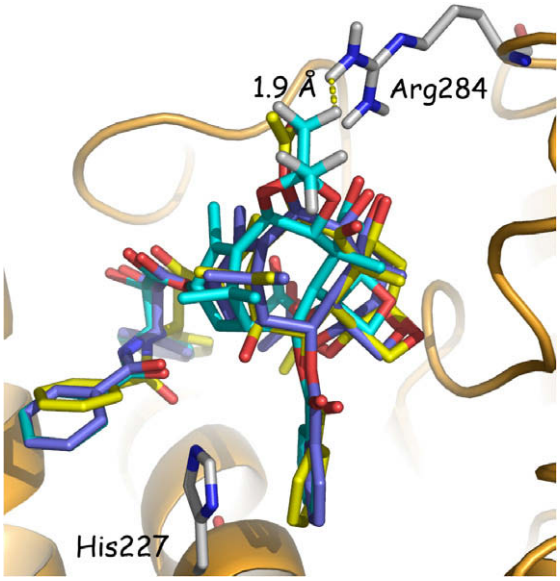

Figure 2. Docking poses of Taxol (yellow), **9** (cyan) and **10** (blue) within the taxane–tubulin binding pocket.

a good predictor for the tubulin binding and bioactivity of taxanes. The results obtained in the present work offer an additional example of its utility and effectiveness.

Acknowledgments

The authors are grateful to the National Natural Science Foundation of China (Projects No. 30672506) and Leading Academic Discipline Project of Shanghai Municipal Education Commission (Project No. J50102). J.P.S. and Y.J. are grateful to the National Institutes of Health Grant CA-69571 for partial support of the work.

A. Supplementary data

Supplementary data associated with this article can be found, in the online version, at doi:10.1016/j.bmcl.2008.12.091.

References and notes

1. Georg, G. I. In *Taxol: Science and Application*; Suffness, M., Ed.; CRC: Boca Raton, FL, 1995; p 317.
2. Guénard, D.; Guéritte-Voegelein, F.; Potier, P. *Acc. Chem. Res.* **1993**, *26*, 160.
3. Gottesman, M. M.; Fojo, T.; Bates, S. E. *Nat. Rev. Cancer* **2002**, *2*, 48.
4. Spletstoser, J. T.; Turunen, B. J.; Desino, K.; Rice, A.; Datta, A.; Dutta, D.; Huff, J. K.; Himes, R. H.; Audus, K. L.; Seelig, A.; Georg, G. I. *Bioorg. Med. Chem. Lett.* **2006**, *16*, 495.
5. Guénard, D.; Thoret, S.; Dubois, J.; Adeline, M.-T.; Wang, Q.; Guéritte, F. *Bioorg. Med. Chem.* **2000**, *8*, 145.
6. Poujol, H.; Mourabit, A. A.; Ahond, A.; Poupat, C.; Potier, P. *Tetrahedron* **1997**, *53*, 12575.
7. Ishiyama, T.; Iimura, S.; Ohsuki, S.; Uoto, K.; Terasawa, H.; Soga, T. *Bioorg. Med. Chem. Lett.* **2002**, *12*, 1083.
8. Lin, H. X.; Li, M.; Chen, J. M.; Chen, M. Q. *Chin. J. Chem.* **2004**, *22*, 751.
9. (a) Chaudhary, A. G.; Chordia, M. D.; Kingston, D. G. I. *J. Org. Chem.* **1995**, *60*, 3260; (b) Chen, S. H.; Huang, S.; Gao, Q.; Golik, J.; Farina, V. *J. Org. Chem.* **1994**, *59*, 1475; (c) Yin, D. L.; Sekiguchi, Y.; Kameo, K. *Chin. Chem. Lett.* **1998**, *9*, 373.
10. Kingston, D. G. I.; Chordia, M. D.; Jagtap, P. G.; Liang, J. Y.; Shen, Y. C.; Long, B. H.; Fairchild, C. R.; Johnston, K. A. *J. Org. Chem.* **1999**, *64*, 1814.
11. See synthetic procedures and characterization data for compounds **6**–**10** in Supplementary data.
12. Dubois, J.; Guéritte-Voegelein, F.; Guedira, N.; Potier, P.; Gillet, B.; Beloeil, J.-C. *Tetrahedron* **1993**, *49*, 6533.
13. (a) Snyder, J. P.; Nettles, J. H.; Cornett, B.; Downing, K. H.; Nogales, E. *Proc. Natl. Acad. Sci. U.S.A.* **2001**, *98*, 5312; (b) Lowe, J.; Li, H.; Downing, K. H.; Nogales, E. *J. Mol. Biol.* **2001**, *313*, 1045.
14. Mastropaolo, D.; Camerman, A.; Luo, Y.; Brayer, G. D.; Camerman, N. *Proc. Natl. Acad. Sci. U.S.A.* **1995**, *92*, 6920.
15. See Fig. S1 and Fig. S2 in Supplementary data.
16. Macromodel 9.0 (Maestro 7.0 interface), supplied by Schrödinger, Portland, OR; www.schrodinger.com.
17. (a) Nogales, E.; Wolf, S. G.; Downing, K. H. *Nature* **1998**, *391*, 199; (b) Jiang, Y.; Alcaraz, A. A.; Chen, J.-M.; Kobayashi, H.; Lu, Y. J.; Snyder, J. P. *J. Med. Chem.* **2006**, *49*, 1891.
18. (a) Friesner, R. A.; Banks, J. L.; Murphy, R. B.; Halgren, T. A.; Klicic, J. J.; Mainz, D. T.; Repasky, M. P.; Knoll, E. H.; Shaw, D. E.; Shelley, M.; Perry, J. K.; Sander, L. C.; Shenkin, P. S. *J. Med. Chem.* **2004**, *47*, 1739; (b) Halgren, T. A.; Murphy, R. B.; Friesner, R. A.; Beard, H. S.; Frye, L. L.; Pollard, W. T.; Banks, J. L. *J. Med. Chem.* **2004**, *47*, 1750.